symmetry

Article

Genetic Algorithm for Optimizing Energy Efficiency in Downlink mmWave NOMA System with Imperfect CSI

Reem Aldebes, Kaharudin Dimyati * and Effariza Hanafi *

Department of Electrical Engineering, Faculty of Engineering, Universiti Malaya, Kuala Lumpur 50603, Malaysia
* Correspondence: kaharudin@um.edu.my (K.D.); effarizahanafi@um.edu.my (E.H.)

Abstract: Nonorthogonal multiple access (NOMA) is considered a promising technique for improving energy efficiency (EE) in beyond-5G wireless systems. In this paper, we investigate the maximization of EE of downlink wireless systems by combining mmWave with NOMA technologies, considering the asymmetric required data rate of user applications. We propose a genetic algorithm (GA) to solve the non-convex energy efficiency problem for an imperfect CSI downlink mmWave NOMA system. The studied mixed-integer optimization problem was converted to an integer optimization problem and solved using a GA, which determines the best clustering members in mmWave NOMA. The required population size of the proposed GA was determined to evaluate its effectiveness for a massive number of users. In addition, the GA's convergence to the optimal solution for light traffic and relatively heavy traffic was also analyzed. Our results illustrate that the solution obtained solution via GA is almost equal to the optimal value and outperforms the conventional orthogonal multiple access, where the EE is improved by more than 75%. Finally, the impact of the estimation error of CSI on the system performance was evaluated at different required SINR scenarios. The results show that EE is degraded in the case of imperfect CSI case but is still close to the optimal solution.

Keywords: energy efficiency; genetic algorithm; imperfect CSI; millimeter wave (mmWave); non-orthogonal multiple access (NOMA)

Citation: Aldebes, R.; Dimyati, K.; Hanafi, E. Genetic Algorithm for Optimizing Energy Efficiency in Downlink mmWave NOMA System with Imperfect CSI. *Symmetry* **2022**, *14*, 2345. https://doi.org/10.3390/sym14112345

Academic Editor: Haitao Xu

Received: 7 October 2022
Accepted: 1 November 2022
Published: 8 November 2022

1. Introduction

With the growing Internet of Things and cloud-based applications, the demand for new services and data traffic for wireless communications increases tremendously. Thus, one of the expectations for 6G is to increase the transmission data rate to achieve a peak value of 1 Tbps to provide a massive number of users with the required service [1]. The accessible spectrum resources are restricted since they serve tens of thousands of pieces of mobile communications equipment and therefore more techniques are required to guarantee the connection quality for each user [2]. NOMA is considered a very promising technique in beyond 5G and 6G where it provides services to several users simultaneously at the same subcarrier and at the same time through the use of superposition coding in the power domain [3]. NOMA has several advantages such as high spectrum efficiency, improved cell edge data rate, low latency, and good compatibility with other techniques such as orthogonal multiple access (OMA) [4]. Moreover, considerable improvements in spectrum efficiency (SE), energy efficiency (EE), and outage probability are achieved in MIMO-NOMA-based communications compared to MIMO-OMA when an appropriate resource allocation is implemented [5]. However, the channels in the massive MIMO systems exhibit a high degree of spatial correlation. In [6], a large-system analysis is applied to the covariance-aided CSI acquisition strategy in the MIMO system, which exploits the individual covariance matrices for channel estimation when non-orthogonal pilot sequences are used. The analysis shows that the training overhead can be reduced when a covariance-aided strategy is implemented compared to the conventional CSI acquisition, where no knowledge of the user spatial co-variance matrices is known.

EE is a significant key when designing future green communication networks [7], especially with the increasing global attention towards energy conservation [8]. Thus, maximizing EE is considered one of the challenges in 6G wireless networks, where enormous power is consumed to provide a massive number of users with 1000 times the data rate [9]. NOMA is typically integrated with other techniques such as millimeter wave (mmWave) to improve energy efficiency by degrading the interference and increasing the data rate [10]. The mmWave bands offer a widely available resource compared to the previous systems that operate on microwave bands, and they also meet the high requirements of data rates and throughput of the wireless communication's users.

2. Related Works

The EE optimization and throughput optimization problems in NOMA have been studied under various constraints such as the total power, interference, and/or minimum quality of service (QoS) of the users. A code reuse scheme in the downlink MIMO-NOMA system that separates active users into groups based on their channel quantity and inner interference is proposed in [11]. The transmitted data correlation matrix is constructed at the transmitter using only the primary eigenvector and eigenvalue of the corresponding correlation matrix as the input via feedback, deducted via principal component analysis. The performance of this scheme is evaluated in terms of code assignment gain and bit error rate. The results show that employing the successive interference cancellation (SIC) technique at the receivers can achieve an improvement over the conventional OMA. On the other hand, the same SINR level is assumed for all users in [12]. Similarly, minimizing the total power consumption of the whole network under the constraint of all users' long-term rate requirements is assumed in [13]. However, applications that require high QoS can drain network resources [14]. Many applications, such as instant messaging, email reading, video streaming, online learning, and online gaming, require asymmetric data rates [15] and therefore more studies should address improving system performance while considering the different equipment of each user.

Many prior works have studied power allocation in NOMA as the key role to optimize EE in perfect channel state information (CSI) cases [16–18]. In a real cellular system, it is a challenge to obtain full CSI at the base station (BS) because of the channel estimation error and the quantization error [19–21]. However, channel estimation errors in the imperfect CSI downlink NOMA system could cause user ordering ambiguities [22]. The pilot transmission design for power-domain NOMA and the influence of the inaccurate channel estimation on power-domain NOMA were investigated in [23]. Previous studies found that NOMA technology has better performance than OMA in the imperfect CSI case. The resource allocation was investigated in [24] for multi-carrier NOMA depending on the available statistical CSI at the transmitter. Moreover, partial CSI was used in [25–27] to determine the order of the user equipment, where CSI feedback is mainly considered a potential improvement to support the BS in sorting user equipment. For example, one-bit feedback from the user to the transmitter scheme is proposed in [27] to indicate whether the sending bit is below or above a specific power level.

In [19], the impact of the CSI error levels on the system performance was investigated and the energy efficiency at various transmission power levels and the channel estimation error were evaluated. The results show that the system performance was improved compared to OMA. Thus, NOMA is recommended for only two users in the cluster to achieve the user's required data rate. The probabilistic problem is converted to a non-probabilistic version in [20] to maximize EE in imperfect CSI downlink NOMA system under outage probability constraints. Since outage probability is one of the maximization problem constraints in [20], the number of served equipment in the cell has to be evaluated. A simple suboptimal user device scheduling mechanism is presented to maximize the system EE and a closed-form formula of the assigned power for two or more users is derived in [21].

Tackling the optimization problem becomes more challenging and complicated especially when dealing with a massive number of users in the beyond 5G and 6G networks.

Solving the non-convex EE maximization via traditional approaches suffers from poor resource utilization, while some advanced techniques that involve fractional programming and sequential convex optimization or heuristic algorithms for targets are unable to find effective solutions to large-scale wireless networks because of the complexity of wireless communication systems [28]. This has motivated the use of artificial intelligence (AI)-based methods to satisfy these massive wireless connectivity requirements and solve power allocation and subchannel problems in the mmWave systems. Machine learning techniques can provide new ideas for intelligent energy-efficient algorithms in wireless networks due to quickly adapting to environmental changes [29]. The authors in [30] adopted the machine learning approach to decide the best user association in the mmWave NOMA system that maximizes EE. To maximize the EE under the constraints of QoS, interference, and transmission power in [31], the authors propose a machine learning framework to deal with the user association, subchannel, and power allocation problems in the NOMA mmWave heterogeneous networks to meet the various requirements of users in different applications. Deep learning trained with genetic algorithms (GAs) is proposed in [32] to make benefits of the advantages of deep learning and genetic algorithm where combining GA with deep learning significantly reduces the computation time of complicated optimization problems in various scenarios. Moreover, the combined algorithm is advisable to solve complicated optimization problems and problems with high required timeliness.

Forming clusters for different channel gain users in the mmWave NOMA system is one of the aspects of achieving a good performance in NOMA. However, an excessive overhead is required to enable the BS to the users' state information in order to form the clusters and allocate the power to each cluster's member that improves the system performance [33]. In [34], a Stackelberg game-based algorithm is proposed to design the user clustering and power allocation that maximizes the sum rate of the mmWave-NOMA system where the CSI of all cluster users is assumed to be perfectly known at the BS. More approaches are required to optimize the EE of the mmWave-NOMA system with a massive number of users considering the imperfection in the channel state.

3. Contribution

We focus on user clustering to maximize the EE in the downlink (DL) mmWave NOMA imperfect CSI system subjected to the asymmetric user data rate requirement using an artificially intelligent method (genetic algorithm) for light traffic and heavy traffic cases. In the field of artificial intelligence, GAs have arisen as a powerful tool to solve the non-convex optimization problem to determine the minimum solutions when the level of quality of service is constrained and the resources are limited, especially when no full information about the user states is available. The major contributions of this paper are:

1. Formulating the energy efficiency optimization problem for DL mmWave NOMA system with user clustering under total power and specific required *SINR* for each user depending on the user applications.
2. Investigating the role that power allocation can play to maximize the energy efficiency in a DL mmWave NOMA system with clustering where the user applications impose asymmetric SINR requirements. For this purpose, the EE of a two-member cluster system is evaluated at asymmetric user requirements scenarios where the cell-edge user and the nearby-BS user require different data rates.
3. Converting the mixed-integer GA problem to an integer GA problem for solving the EE optimization problem by determining the best clusters.
4. Evaluating the performance of GA and its convergence in the case of light traffic and heavy traffic.
5. Comparing the performance of the proposed GA with the optimal solution and the conventional OMA at different user *SINR* requirement scenarios. The results reveal that GA can detect close-to-optimal solutions for a various number of users and user requirements. Additionally, the results show the outperformance of NOMA using the proposed GA algorithm compared to the conventional OMA.

6. Evaluating the impact of estimation error in CSI at BS on the system performance based on the proposed GA and the optimal NOMA. The simulation results show that the GA solution is close to the optimum. However, the EE of the system degrades in the presence of the imperfection of CSI.

The rest of this paper is organized as follows: The system model of cellular downlink NOMA system with imperfect CSI and the EE optimization problem that aims to maximize the EE of the mmWave DL system subject to the required QoS and limited transmission power is presented in Section 4. In Section 5, we detail the proposed genetic algorithm that is used to solve the EE optimization problem with integer unknowns. In Section 6, we present detailed simulation results for the proposed algorithm, including a comparison of the optimal EE to the solution of GA to prove its effectiveness in deciding the optimal sub-channel users in the system and analysis of the impact of imperfection in CSI at the BS on the system performance. Finally, Section 7 concludes the paper. Table 1 lists the notations used in this paper.

Table 1. List of parameters.

Notation	Parameters
θ_m^b	The beam width of the mmWave BS b *to user* m
φ_m^b	The boresight angle from mmWave BS b to user m
γ_m^b	The spatial angle from user m to mmWave BS b
g_m^b	The gain of the directivity between the beam from mmWave BS b to user m and the beam from device m to mmWave BS b
θ_m^u	The beam width of the user m to mmWave BS b
φ_m^u	The boresight angle from device m to mmWave BS b
γ_m^u	The spatial angle from mmWave BS b to user m
g_m^u	The gain of the directivity between the beam from user m to mmWave BS b and the beam from mmWave BS b to user m
g_m^c	The gain of the channel linked the user m to the mmWave BS b
ϵ	Side lobe
h_m	The complete representation of the channel between BS b and user m
p_m	The allocated power to the user m from the mmWave BS b

4. System Model and Problem Formulation

In this study, a single-cell cellular NOMA mmWave system is considered as illustrated in Figure 1, where the beamforming-based directional links are considered [30,35]. The central BS is equipped with multiple antennas, whereas each user is equipped with a single antenna. Without losing generality, the users are assumed to be uniformly allocated [30]. The set of users within the cell boundary is $\mathcal{M} = \{1, 2, 3, \ldots, M\}$. The set of the clusters is denoted as $\mathbb{C} = \{1, 2, 3, \ldots, C\}$ where one subchannel is dedicated for each cluster. The user association state between every user and BS is represented by the $X^{M\times B}$ matrix as follows:

$$X = \begin{bmatrix} x_{1,1} & \cdots & x_{1,B} \\ \vdots & \ddots & \vdots \\ x_{M,1} & \cdots & x_{M,B} \end{bmatrix} \quad (1)$$

where $x_{m,b} = 1$ when the user m is a member of cluster b, and $x_{m,b} = 0$ when it is not. Due to the complexity of SIC decoding, we assumed that each cluster can support two members simultaneously on one subchannel [36].

The gain of the directivity between the beam from the mmWave BS to user m and the beam from user m to the mmWave BS is given by

$$g_m^b\left(\theta_m^b, \varphi_m^b, \gamma_m^b\right) = \begin{cases} \epsilon, & if\ \frac{\theta^b}{2} < \left|\varphi_m^b - \gamma_m^b\right| < 2\pi - \frac{\theta^b}{2} \\ \frac{2\pi-\left(2\pi-\theta^b\right)\epsilon}{\theta^b}, & otherwise \end{cases} \quad (2)$$

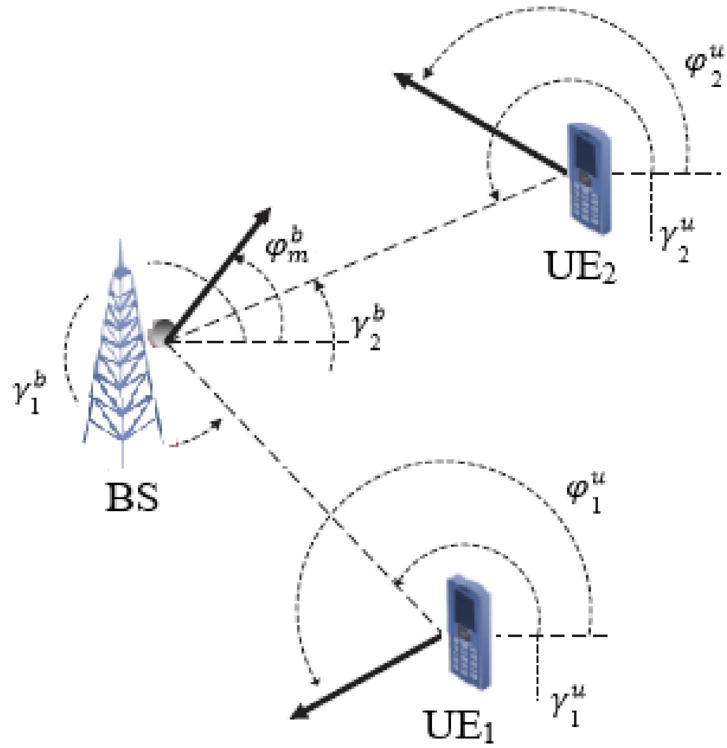

Figure 1. The proposed DL mmWave NOMA system.

Similarly, the gain of the directivity between the beam from user m to the mmWave BS and the beam from the mmWave BS to user m is given as

$$g_m^u({\theta_m}^u, \varphi_m^u, \gamma_m^u) = \begin{cases} \epsilon, & if\ \frac{{\theta_m}^u}{2} < |\varphi_m^u - \gamma_m^u| < 2\pi - \frac{{\theta_m}^u}{2} \\ \frac{2\pi - (2\pi - {\theta_m}^u)\epsilon}{{\theta_m}^u}, & otherwise \end{cases} \tag{3}$$

The cluster users are supported at the same time and at the same subchannel by utilizing superposition coding techniques. The channel gain from the BS to every user is given by $g_m^c = c_m {d_m}^{-\frac{\delta}{2}}$, where $c_m \sim CN(0,1)$ is a Rayleigh fading factor, d_m denotes the distance from each UE to the transmitter, and δ refers to the path loss exponent [19]. In practice, it is difficult to attain perfect channel state information due to various reasons such as channel estimation errors, feedback delays, and quantization errors. Here, we consider a NOMA system with imperfect CSI in which the channel estimation is given by $g_m^c = g_m^{\hat{c}} + \varepsilon$, where $\varepsilon \sim CN(0, \sigma_\varepsilon^2)$ is the error of the channel estimation with variance σ_ε^2, and $g_m^{\hat{c}}$ is the estimated channel gain $g_m^{\hat{c}} \sim CN\left(0, \sigma_{\hat{g}_m}^2\right)$ which is uncorrelated with ε [19]. Thus, the complete representation of the channel between the BS and user m is given by:

$$h_m = g_m^b g_m^u g_m^c \tag{4}$$

In the downlink NOMA system, user equipment is ordered according to channel strength ($|h_M| \geq |h_{M-1}| \geq \ldots \geq |h_2| \geq |h_1|$) [22]. Thereby, the SIC technique could extract a specific signal from the superposed signals on a single carrier. The strongest user device is indicated as $\mathrm{UE_M}$ and the weakest user device is indicated as $\mathrm{UE_1}$. The BS transmits M different messages on the same carrier within the same bandwidth. On the other side, each user receives a composition of its message with the interferences from the signals of other users [37]. Figure 2 illustrates the SIC technique in the mmWave-NOMA system where each cluster consists of two members and is carried on a specific subchannel. The mmWave BS in the NOMA system utilizes superposition coding techniques to serve several users simultaneously. A superposed transmitted signal by the mmWave BS can be expressed as [19]:

$$f = \sum_{m=1}^{M} \sqrt{\alpha_m P_{tot}}\, f_m(t) = \sum_{m=1}^{M} \sqrt{p_m}\, f_m \tag{5}$$

where f_m is the individual signal dedicated to the m-th user and $E\{|f_m|^2\} = 1$ before transmission, M is the number of the UEs supported by the mmWave BS, P_{tot} is the total transmitted power of the mmWave BSs, and α_m is the power coefficient allocated to the m-th UE where:

$$\sum_{\forall m \in M} \alpha_m \leq 1 \tag{6}$$

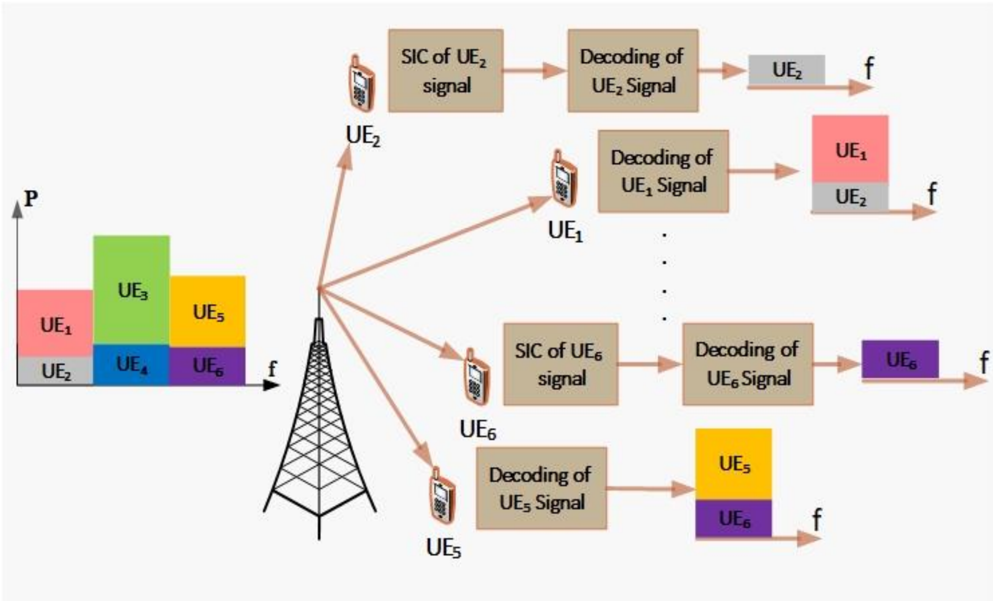

Figure 2. SIC technique to decode signals for two member clusters in DL mmWave-NOMA system.

The variation in the power levels of the composed signals plays an important role in maximizing the cell throughput and EE [38]. The mmWave BS transmits different signals over the same frequency resource while every user receives its desired signal combined with the interferences due to the other users' signals on the same radio signal [37]. Each one of the downlink NOMA's users undergoes a different attenuation according to its channel gain with the mmWave BS. The user with the strongest channel has the capability to decode the signals of the remaining users before decoding its own signal. On the other hand, the user with the weakest channel cannot eliminate the signals of the other strong channel UEs. The received signal at the m-th UE terminal before applying the SIC technique is given by [19]:

$$y_m = \sum_{\forall l \in M, b \in B} \sqrt{x_{m,b} g_m^b g_m^u g_m^c p_l} f_l + w_m \tag{7}$$

where p_l is the allocated power to the l-th user and w_m represents the additive white Gaussian noise (AWGN). In general, the signal after applying SIC technique at the m user can be expressed as [19]

$$y_m = \sqrt{x_{m,b} g_m^b g_m^u g_m^c p_m} f_m + \underbrace{\sum_{\forall l \in M} \sqrt{x_{m,b} g_m^b g_m^u g_m^c p_l} f_l}_{l>m} + \sum_{\forall l \in M} \sqrt{\varepsilon x_{l,b} p_l} f_l + w_m \tag{8}$$

where in Equation (8), the dedicated signal for the m-th UE is represented by the first term, while the second term is the inter-channel interference due to decomposed signals on the same subchannel of other users and the third term is due to the estimation error of the CSI. It is worth mentioning that the interference due to the signals of the other clusters will be eliminated by filtration where other clusters are on different subchannels.

It is assumed that all users utilize the mmWave spectrum resources completely to achieve full employment of the directional gain of the mmWave system. Thus, the communication link between the mmWave BS and the m-th user is subjected to interference given by

$$I_m = \underbrace{\sum_{\forall l \in M} x_{m,b} p_l g_m^b g_m^u g_m^c}_{l<m} + \sigma_\varepsilon^2 \sum_{l=1}^{M} x_{l,b} p_l \tag{9}$$

This is considered a commonly used interference model in mmWave power allocation system [39]. Based on the interference model, the signal-to-interference ratio (SINR) at the m-th user is given as

$$SINR_m = \frac{x_{m,b} p_m g_m^b g_m^u g_m^c}{I_m + BN_o} \tag{10}$$

where B represents the utilized bandwidth and N_o represents the power spectrum density of the AWGN at the user terminal. Thereby, the obtained data rate at the m-th user from the mmWave BS can be expressed as

$$R_m = Blog_2(1 + SINR_m) \tag{11}$$

The improved throughput is an advantage of the NOMA over the conventional OMA. For a more specific comparison, conventional frequency division multiple access (FDMA) will be considered in this paper. For a fair comparison with the NOMA, the bandwidth dedicated for each cluster is divided equally among its members so that the cluster will support the same number of users within the same dedicated bandwidth in both systems, NOMA and OMA. Thus, the data rate of the m-th user from the mmWave BS in OMA system is determined as

$$R_m^{OMA} = \frac{B}{M} log_2\left(1 + \frac{\sum_{n \in N} P_m g_m^b g_m^u g_m^c}{\sigma_\varepsilon^2 P_m + \frac{B}{M} N_o}\right) \tag{12}$$

The advantage of NOMA over OMA in increasing the data rate can be illustrated by taking an example of a cell with only two users where the first is at the cell edge, which is far from the BS, while the second is near the BS. Although low power will be allocated to the nearest user who has the strongest channel, its *SINR* will be high since no inter-cell interference significantly affects it.

Due to the system's resource constraints, the number of served users and their allocated power should be determined carefully to ensure the QoS of wireless systems. Furthermore, the difference in the allocated power levels should be verified so that each receiver is able to perform SIC and extract the desired signal [37]. The sum data rate of the NOMA mmWave downlink system is expressed as

$$R_{sum} = \sum_{m \in M} R_m \tag{13}$$

Based on the given data rate, the energy efficiency of the user association NOMA mmWave downlink system can be written as [40]

$$EE = \frac{R_{sum}}{\sum_{m \in M} p_m + P_c} \tag{14}$$

where P_c represents the circuit power dissipation for SIC detection at the mmWave BSs where we assumed that it is fixed for all users. In this work, we aim to maximize the non-concave EE optimization problem of the NOMA mmWave with clustering. The power allocated by the mmWave BS to each user depends on the required QoS by that user within the limited total BS transmission power. Each cluster is assumed to consist of two members while each user is supported by one cluster (subchannel). We aim to find the optimal cluster composition that maximizes the EE of the mmWave system subjected to the required QoS and limited transmission power. This EE optimization problem can be formulated as

$$\begin{aligned} &\underbrace{\max}_{x_{m,b},p_m} \; EE = \frac{R_{sum}}{\sum_{m\in M}\sum_{b\in B} x_{m,b}p_m + P_c} \\ &subject\ to\ \ C1: \ x_{m,b} \in \{0,1\}, \ \ \forall m \in M, \ \forall b \in B, \\ &C2: \sum_{m\in M,\ \ b\in B} x_{m,b} = 1, \ \ \forall m \in M, \\ &C3: \sum_{m\in M,\ b\in B} x_{m,b} = 2, \ \ \forall b \in B, \\ &C4: \sum_{m\in M}\sum_{b\in B} x_{m,b}p_m \le P_{tot}, \\ &C5: \ SINR_m \ge \delta_m, \ \ \forall m \in M \end{aligned} \tag{15}$$

where $C1$ refers to the association of each user m with a cluster b. $C2$ states that each user should be supported by one cluster while $C3$ defines every cluster as consisting of two members. The limited transmission power of the mmWave BS is represented in $C4$ while $C5$ is to ensure that the minimum QoS requirements for all users in the DL mmWave NOMA system are satisfied. We will discuss a mechanism to allocate the power to the cluster members in Section 3.

The difficulties and complexity of finding all x_{mn} and p_m that maximize the data rate in the downlink user association mmWave NOMA system are obvious. In addition, the relation between the data rate and the transmitted power makes this problem a non-convex optimization problem that is difficult to solve using classical methods. Therefore, here we employed the genetic algorithm to solve the subchannel association problem. Based on the GA scheme, the optimization problem in (15) is a mixed integer nonlinear problem.

5. Power Allocation and GA Scheme

5.1. Power Allocation

To propose a mechanism to allocate the power to cluster members of various required data rates, first we will investigate the assumption of allocating higher power to the weaker-channel state user in the cluster as well as the assumption that allocating the lower power to the stronger-channel state user is required to ensure that higher EE can be achieved [41]. For simplicity, we consider a simple scenario where the mmWave has complete CSI information of all users. Thus, for a two-member cluster, the *SINR* of the strong-channel user ($SINR_1$) and the *SINR* of the weak-channel user ($SINR_2$) are given as:

$$SINR_1 = \frac{p_1 g_1^b g_1^u g_1^c}{p_2 g_1^b g_1^u g_1^c + BN_o} \tag{16}$$

and

$$SINR_2 = \frac{p_2 g_2^b g_2^u g_2^c}{BN_o} \tag{17}$$

where the SIC technique is used at the UE_2 to eliminate the interference due to the weaker-channel user UE_1. Assuming a unity channel gain, $h_2 = 1$, and the required QoS of the UE_2 is 2, the allocated power p_2 would be 2 regardless of the UE_1 requirement. On the other hand, the allocated power to the weak-channel user UE_1 (p_1) would be less than (p_2) when its QoS requirement is only at low levels. However, when UE_1 requests a higher data rate, its allocated power should be higher than the allocated power of UE_1. Figure 3 illustrates the allocated power and the EE for a cluster of 2 members with various requirements and channel states. As can be seen from Figure 3, the weaker channel user requires higher allocated power to achieve the data rate. Although previous studies have found that increasing the allocated power to the strong-channel user significantly increases the total throughput of the system, this rise of the allocated power decreases the system EE based on Equation (14).

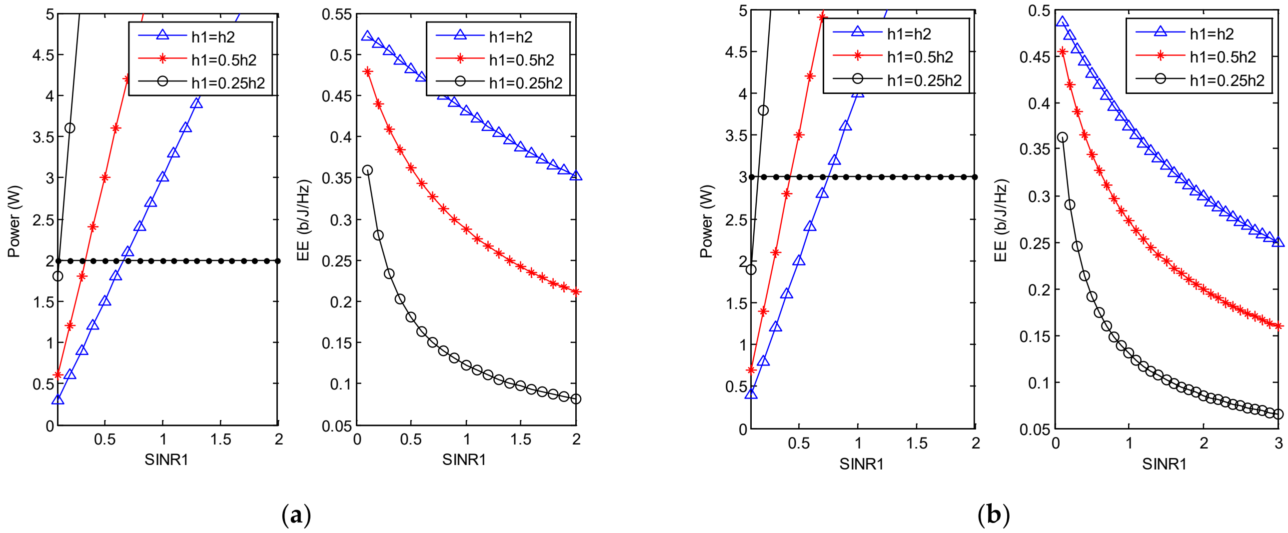

Figure 3. The allocated power to the two members of the cluster and the EE vs. the obtained SINR at the weaker-channel user (h_1) when the required SINR of the stronger-channel user (h_2) is 2 in (**a**) and 3 in (**b**). (**a**) $SINR_2 = 2$; (**b**) $SINR_2 = 3$.

The question here is whether increasing the data rate of the strong-channel user (UE_2) in the cluster higher than its requirements will be a benefit to the system EE. To answer this question, the allocated power to the strong-channel member in the cluster is increased so that its new *SINR* is 3, as seen in Figure 3b. This leads to a noticeable increment in the power allocated to the weaker-channel user to attain its requirement, and eventually the system EE degrades. Thus, the best scenario to achieve the highest EE to support the cluster members with the same requirements of data rate is to set the subject *C*5 in the optimization problem as $SINR_m = \delta_m$.

In this study, we assumed that the power allocated to every user will satisfy the user's QoS (δ_m). We then studied the possibility of improving the system EE by selecting different members in the cluster. Assume there are two weak-channel users in the cell. We refer to the user with $h_1 = 0.5h_2$ as UE_x and refer to the user with $h_1 = 0.25h_2$ as UE_y. The general assumption of selecting either one of them as a second member in the cluster depends on its channel state; increase in the system EE is not an accurate conclusion when, as seen in Figure 3a, the required QoS of every user plays an important role in this issue. For example, choosing UE_x leads to higher EE when the required *SINR* of UE_x is $\delta_x = 0.5$ and the required *SINR* of UE_y is $\delta_y = 0.5$, while choosing UE_y leads to higher EE when $\delta_x = 2$ and $\delta_y = 0.25$.

Although selecting the cluster members with various QoS requirements can be decided easily in this example, the massive number of users in real wireless communication networks makes the problem more complicated, as there are $\frac{M!}{2!(M-2)!}$ different combinations of 2 members in a cell of *M* users [42], and therefore we adopted a GA scheme in this study to determine the optimal cluster combinations $x_{m,b}$ to maximize the EE of the DL mmWave NOMA system.

5.2. Genetic Algorithm

Genetic algorithms (GAs) are one of the classical heuristic algorithms that have been successfully implemented to solve non-convex optimization problems [43]. In this section, we describe the components of the genetic algorithm to solve the EE optimization problem in downlink mmWave NOMA with clustering.

GAs are one of the evolutionary algorithms inspired by the biological selection process, and they follow similar operators. Goldberg's genetic algorithm was inspired by Darwin's evolution theory, which says that an organism's survival is determined by the criterion "the strongest species survive". Based on Darwin's theory, an organism's survival can be ensured by the processes of reproduction, crossover, and mutation [44]. His principle of evolution is utilized later in a computational algorithm to solve a problem called an objective function. The solution found via GA is indicated by a chromosome and a collection of chromosomes represents a population. A chromosome comprises genes, and the value of each chromosome can be numerical, binary, or character depending on the nature of the problem. These chromosomes pass through a series of steps starting with a fitness function process to evaluate the suitability between the solution provided via GA and the problem. Through another process called a crossover, new offspring of chromosomes are generated by mating some chromosomes in the population. The genes carried by the new offspring are a mixture of their parents [45]. On the other hand, some chromosomes in the generation will undergo gene mutation. The crossover rate and mutation rate values determine the number of chromosomes that will undergo crossover and mutation, respectively. According to Darwin's rule of evolution, the chromosome with the highest fitness value will have a larger chance of being selected again in the future generation. The chromosomal value converges over numerous generations to a specific value that is the optimal solution for the problem [14].

By utilizing GA to solve the problem in Equation (15), repetitively assigning cluster members and determining their PA process should be performed to determine the maximum EE. Based on the known CSI of the users at the mmWave NOMA BS, the allocated power to the weaker-channel user and the allocated power to the strongest user depend on their inquired QoS to attain $C5$. To solve the non-convex optimization problem in Equation (15) using GA, a reformulation was conducted to achieve a minimization problem, which can be written as

$$\begin{aligned} &\underbrace{\min}_{x_{m,b}} - \frac{R_{sum}}{\sum_{m\in M}\sum_{b\in B} x_{m,b}p_m + P_c} \\ &subject\ to\ \ C1:\ x_{m,b} \in \{0,1\},\ \ \forall m \in M,\ \forall b \in B, \\ &C2:\ \sum_{m\in M,\ \ b\in B} x_{m,b} = 1,\ \ \forall m \in M, \\ &C3:\ \sum_{m\in M,\ b\in B} x_{m,b} = 2,\ \ \forall b \in B, \\ &C4:\ \sum_{m\in M}\sum_{b\in B} x_{m,b}p_m \leq P_{tot}, \\ &C5:\ SINR_m = \delta_m,\ \ \forall m \in M \end{aligned} \tag{18}$$

An integer GA was utilized to determine the best cluster combination that maximizes EE. The GA process to solve the optimization problem in Equation (18) consists of sequential stages that begin with a determination of the chromosome number, maximum number of generations, mutation rate, and crossover rate. Initial values of x_{mb} are assumed, then sequences of selection and mutation are performed. The evolution starts with random individual elements $x_{m,b}$ of the generation that satisfy $C1$, $C2$, and $C3$. Based on $C2$, the sum of each row in the matrix X in Equation (1) should equal 1, which indicates that each user is supported by only one subchannel via one cluster in the cell. On the other hand, based on $C3$, the sum of each column in X should be equal to 2 since each cluster supports 2 members. Because these are integer constraints, the linear equality constraints of the optimization problem in Equation (18) should be reformulated to inequality constraints. Generally, the vector form for the linear inequality constraints of a GA problem is given as

$$AX \leq b \tag{19}$$

For a problem of n_c linear inequality constraints and n_{vars} variables, A is a matrix of size n_c-by-n_{vars} and b is a vector of length n_c. Thus, $C2$ and $C3$ can be reformulated as

$$C2:\begin{cases}\sum_{b=1}^{B} x_{m,b} \leq 1\\ \sum_{b=1}^{B} x_{m,b} \geq 1\end{cases},\ \forall m \in M, \tag{20}$$

$$and,\ \ C3:\begin{cases}\sum_{m=1}^{M} x_{m,b} \leq 2\\ \sum_{m=1}^{M} x_{m,b} \geq 2\end{cases},\ \forall b \in B \tag{21}$$

Since each cluster is assumed to support 2 users ($B = \frac{M}{2}$), the number of variables n_{vars} would be $\frac{M^2}{2}$ and the number of linear inequality constraints n_c would be $3M$. It is worthy to mention that the initial population created by GA contains several individuals that lie within the preset initial range. For the concerned GA problem, all individuals should lie within the range [0; 1]. Because of the massive number of users in the real wireless system, the population size will contain thousands of potential solutions and the initial population will be randomly selected. The population size of the integer GA problem should be higher than the double GA problem to ensure a feasible solution can be obtained [46].

These generation elements are reproduced iteratively within a maximum number of generations. Providing lower and upper bounds for all $x_{m,b}$ elements is necessary to find the best solution to the integer GA problem. Thus, the lower bound L_b and the upper bound U_b of the problem in Equation (18) are given by:

$$L_b = \begin{bmatrix} 0 & \ldots & 0 \end{bmatrix}_{1 \times n_c} \tag{22}$$

and

$$U_b = \begin{bmatrix} 1 & \ldots & 1 \end{bmatrix}_{1 \times n_c} \tag{23}$$

Some genes of selective individuals in the current population (parents) are passed on to the next generation (children). Usually, the selected individuals are those who have the best fitness values. The other individuals pass through crossover and mutation processes that are illustrated in Figure 4. Thus, the next generation is classified into three types:

- Elite children: Individuals that attain the best fitness values and therefore have a higher probability to appear in the next generation. In the concerned GA problem, the elite group is selected as the individual clustering groups $x_{m,b}$ that attain the maximum EE among the whole population. The percentage of the elite to the total population of individuals is set to 2% to pass completely to the next generation.
- Crossover children: Individuals that are created by mixing the vectors of a pair of parents.
- Mutation children: Individuals that are created by applying random changes, or gene mutations, to individual parents to produce children. The mutation rule applies to the individual with a lower probability to attain maximum EE.

The flowchart of the proposed GA is illustrated in Figure 5 where the fitness of the population units is assessed using the objective function value of the optimization problem in every generation. However, the integer genetic algorithm seeks to minimize a penalty function instead of the objective function. The penalty function adds a term for solution infeasibility to the original objective function [47]. The penalty function consists of weighted penalty parameters to estimate the infraction of the constraints. Thus, the constrained problem is converted to a series of unconstrained problems where their solutions are converged to the potential solution of the original problem. The penalty function represents the fitness function if the candidate solution is feasible. Otherwise, the sum of the constraint violations of the (infeasible) point is added to the objective function [48]. Thus, the penalty function of EE optimization problem in Equation (18) is given as:

$$\underbrace{\min}_{x_{m,b}} - \frac{R_{sum}}{\sum_{m\in M}\sum_{b\in B} x_{m,b} p_m + P_c} + \rho_k \sum_{i=1}^{2} g_i(x), \tag{24}$$

where ρ_k is the penalty factor and the second term in (24) represents the penalty function, which can be represented as

$$g_1(x) = \max\left(1, \sum_{b=1}^{B} x_{m,b}\right), \quad \forall m \in M \tag{25}$$

and

$$g_2(x) = \max\left(2, \sum_{m=1}^{M} x_{m,b}\right), \quad \forall b \in B \tag{26}$$

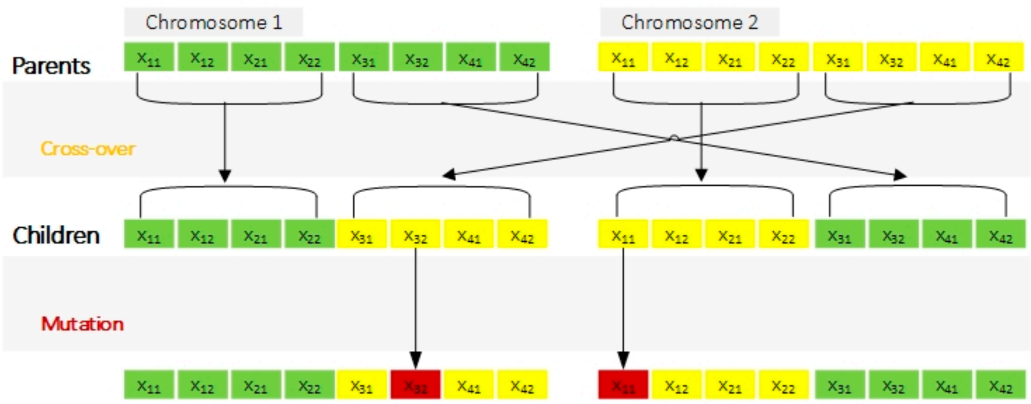

Figure 4. Three classifications of the next generation (children) were created via GA.

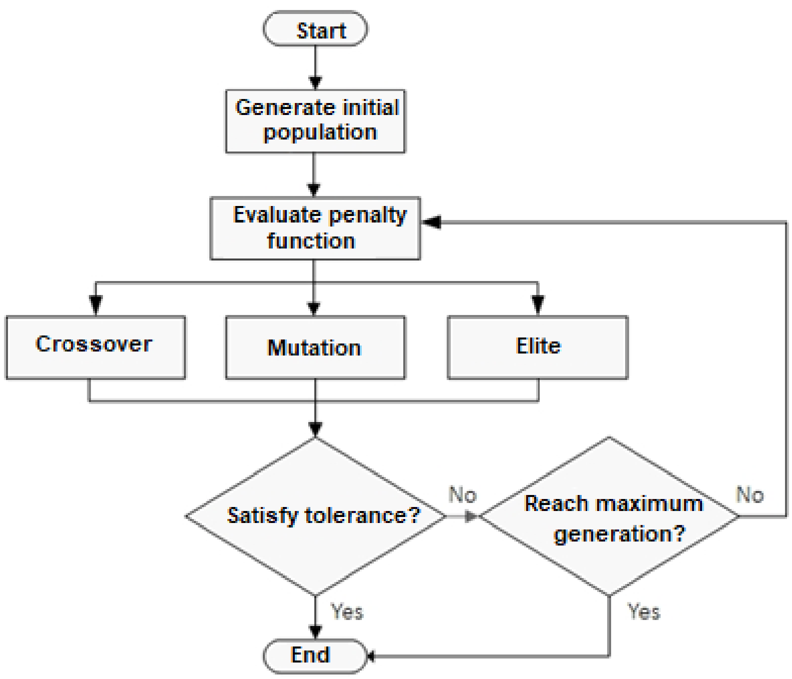

Figure 5. The flowchart of the proposed genetic algorithm.

Initially, the penalty factor is set to a small value, and then it is increased in the next iterations. It is obvious that the penalty function converges to the fitness function when the penalty function attains the constraints. Eventually, the solutions of the successive unconstrained problem will meet the solution of the original constrained problem.

6. Simulation Results

In this section, we will first evaluate the performance of the proposed GA scheme for optimizing the EE in the DL mmWave NOMA system with user clustering. Next, the validity of the proposed scheme is verified by evaluating the performance of the NOMA system in terms of EE and comparing it to both optimal NOMA and conventional OMA.

The general scenario for the simulation is a single cell of a 500 m radius. A mmWave BS with 40 dBm power capability is located at the cell's center and equipped with multiple antennas while M users are distributed randomly at distances between 50 m to 500 m from the mmWave BS within the cell's boundary. The capacity of each cluster is only two users. For simplicity, the transmission beams between the mmWave and the users are assumed to have the same direction, which matches the geographical bore-sight links between them [30]. The allocated power to each user is determined based on its required data rate. The minimum level δ_m is set randomly between 1 and 2. The parameters of the DL mmWave NOMA simulation are listed in Table 2 [30].

Table 2. Simulation Parameters.

Parameter	Value
Operating frequency	24 GHz
Cell radius	500 m
Minimum distance between user and BS	50 m
Required data rate	1–2 b/s/Hz
Total dissipated power at the transmitter	1 Watt
Path loss component	3
BS transmission power	40 dBm
The subchannel bandwidth	1 MHz
AWGN power	−173 dB/Hz
Operating beam-width of the mmWave BS	5°
Operating beam-width of the user	10
Side lobe gain	0.1
Simulation trials	1000
Maximum generations	100
Elite ratio	5% of the population size
Population initial range	[0; 1]
Tolerance of objective function	10^{-12}

6.1. Genetic Algorithm Performance

In this section, the performance of the GA to solve the EE optimization problem in a DL mmWave NOMA system is evaluated. First, diverse population sizes were tested to determine the most appropriate population for different numbers of users. Starting from two clusters (four users) up to eight clusters (sixteen users), the population size was increased until all constraints were satisfied to determine the required population size in relation to the number of users. The elite ratio was 5% of the overall population and the crossover fraction was set to be 50% of the chromosome.

Figure 6 illustrates the required GA population size for various traffic cases. The results illustrated show that the required size of the population in GA is relatively low at light traffic in the cell. As the number of users increases, the minimum population size that guarantees the finding of a feasible solution and satisfies the constraints also increases. The significant increase in the population size indicates a much longer time required to solve the GA. Thus, for a DL mmWave-NOMA with clusters that consist of a massive number of users, GAs could be utilized to determine the optimal cluster pairs that maximize the EE;

however, there is a possibility that this may not satisfy the timeliness requirement. That being said, since GA execution time is much shorter than the required time to evaluate the EE of each possible cluster and determine the optimal solution among all possibilities, the obtained solutions by GA are useful to provide training data for deep learning. The combination between deep learning and GA can improve the solving process by mixing the advantages of the two algorithms, which are determining the near-to-optimal solution (GA) and satisfying the timeliness requirement (deep learning) [32].

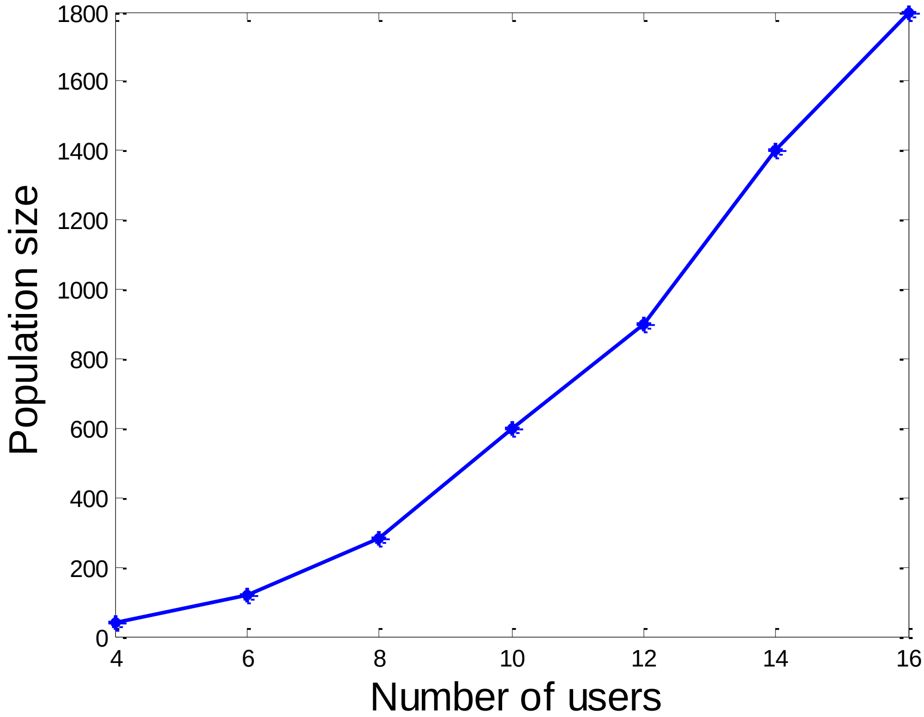

Figure 6. The appropriate population size of the GA with respect to the number of users.

The performance of the GA convergence is evaluated in terms of the relation between the population size and the number of required iterations (generations) to find the solution. For this purpose, two cases were selected: the first case considers relatively low traffic (6 users) while the second case considers relatively heavy traffic (16 users). The results are illustrated in Figures 7 and 8, which show that generally fewer iterations (generations) are required for convergence when the population size is larger for M = 6 users and M = 16 users, respectively. As seen in Figure 7a,b, the convergence to the solution becomes sharper after nine generations and six generations, where the population size increased from 120 to 160. Similar trends can be seen in Figure 8a,b when the population size increases from 1500 to 1800. Moreover, by comparing the results in (a) and (b) for both cases shown in Figures 7 and 8, it is obvious that the number of repetitions (generations) to find the solution reduces when the population size increases. The number of generations executed to solve within the tolerance increases significantly in the case of 16 users as compared to 6 users, and thus this leads to the long execution time of the GA as is shown in Figure 6.

6.2. Impact of the Required SINR

The effect of the users' asymmetric required SINRs on the EE of the proposed system was investigated. The simulation settings remain as in the previous section while the total transmission power is sufficient to provide all users with the required QoS. In the first scenario, we assume a random requirement of user data for different types of applications since some of the applications, such as email, require a much lower data rate than online gaming or video conference. Figure 9a shows the system's EE based on random required SINR, ranging between 1b/s/Hz and 2b/s/Hz for a different number of users. Then, we assume that all users hypothetically have the same requirements, either low SINR (1b/s/Hz) or high SINR (2b/s/Hz), and the results are shown in Figures 9b and 9c, respectively. It can be seen from the figures that the GA approach achieves almost the optimal solution in all cases, which shows its effectiveness for solving complex EE optimization problems. It is obvious that for all cases, the EE degrades as the number of users increases. However, as the number of users increases, the EE of the system approaches the same value for the random SINR requirements and the high SINR cases. Finally, the results show the outperformance of the combination of NOMA with mmWave to improve the system EE compared to OMA-mmWave where a 75% increase in EE can be obtained. For example, the EE rises from about 1b/Joule in mmWave-OMA for 16 users to 2b/Joule in mmWave-OMA under the same circumstances.

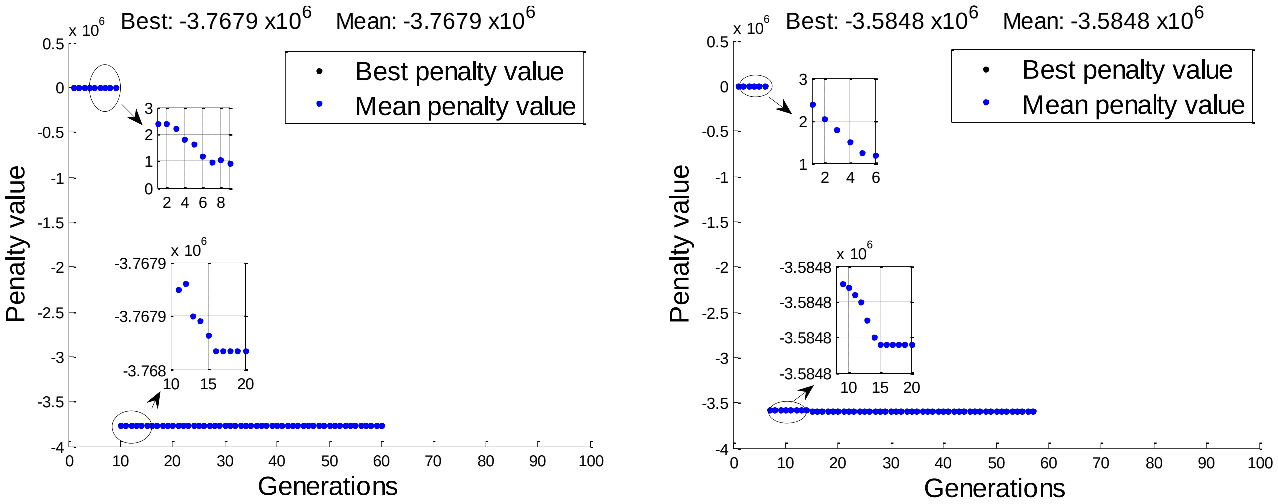

(**a**) (**b**)

Figure 7. The GA convergence to the best penalty value for light traffic case (M = 6). (**a**) Population size = 120. (**b**) Population size = 160.

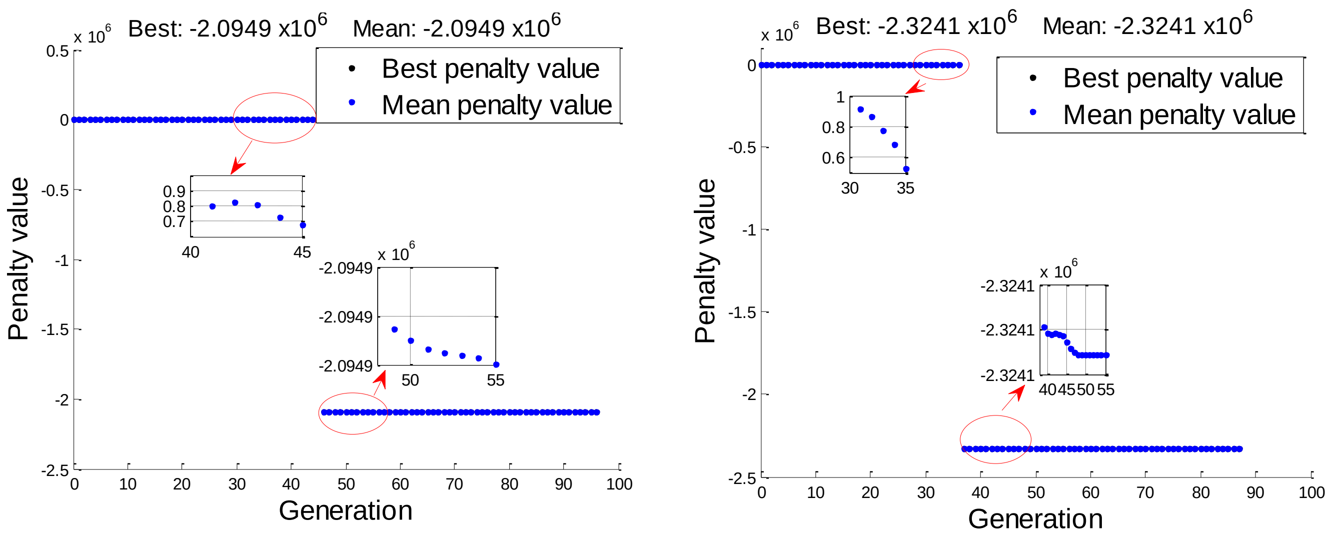

(**a**) (**b**)

Figure 8. The GA convergence to the best penalty value for relatively heavy traffic case (M = 16). (**a**) Population size = 1500. (**b**) Population size = 1800.

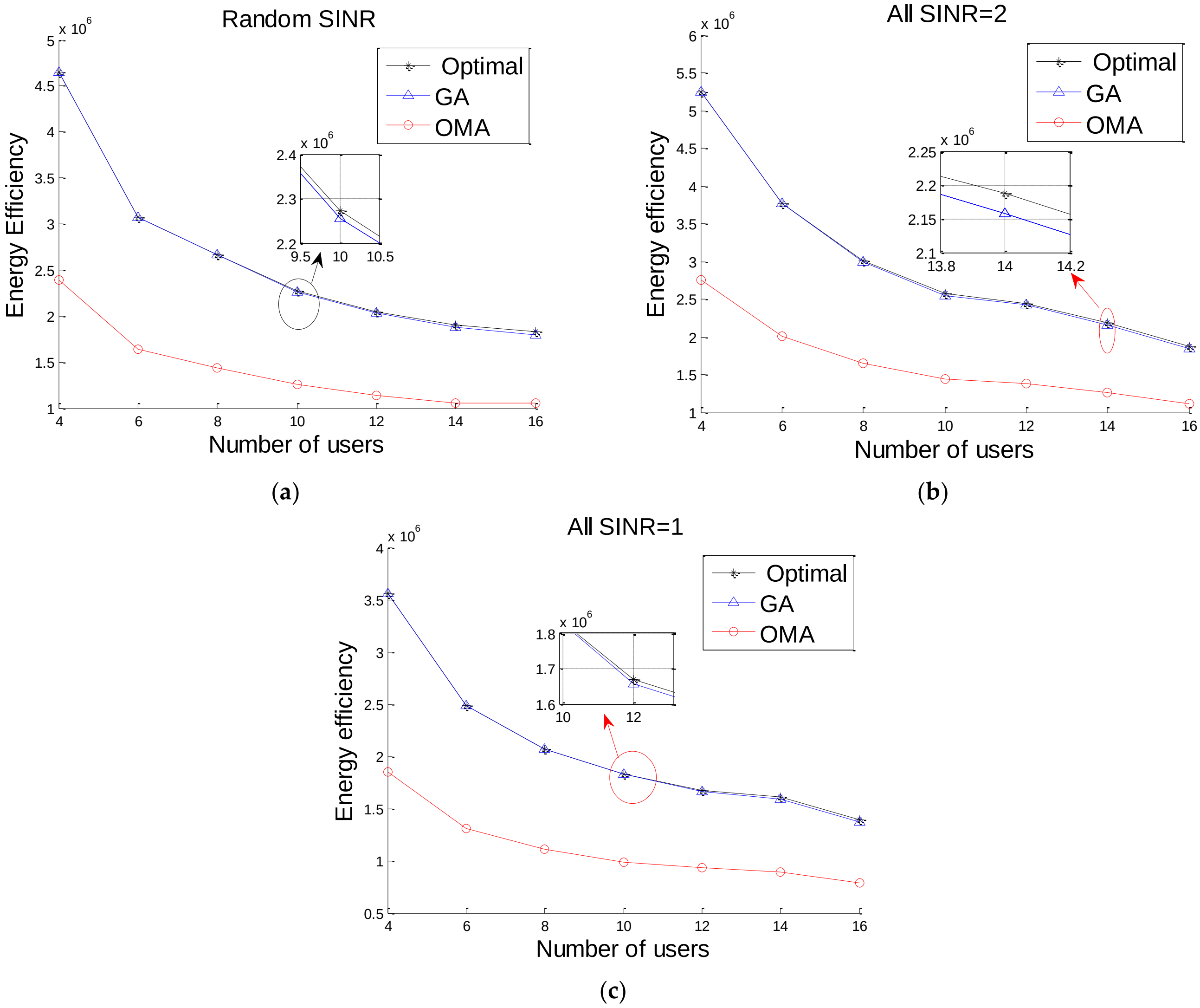

Figure 9. The EE of mmWave-NOMA system versus the number of users at different SINR conditions. (**a**) Random SINR between 1 and 2. (**b**) All SINR = 2. (**c**) All SINR = 1.

6.3. Imperfect CSI

Here, we utilized GA to determine the EE of the mmWave-NOMA system in an imperfect CSI DL mmWave-NOMA system. The effect of the channel estimation error variance on EE for various amounts of user equipment is shown in Figure 10. The number of users is varied from 4 users to 16 users, and channel estimation error σ^2 is set to 0.01. It is evident that the maximum EE is obtained at zero error (perfect CSI), and the channel estimation error causes a decrease in EE because of the decrease in the SINR level. A degradation in the system's performance occurs in the case of imperfect CSI due to the impact of additional noise related to the channel estimation error variance. As can be seen from Figure 10, the performance of the mmWave-NOMA system is better than the conventional OMA system in the imperfect CSI case when GA is employed.

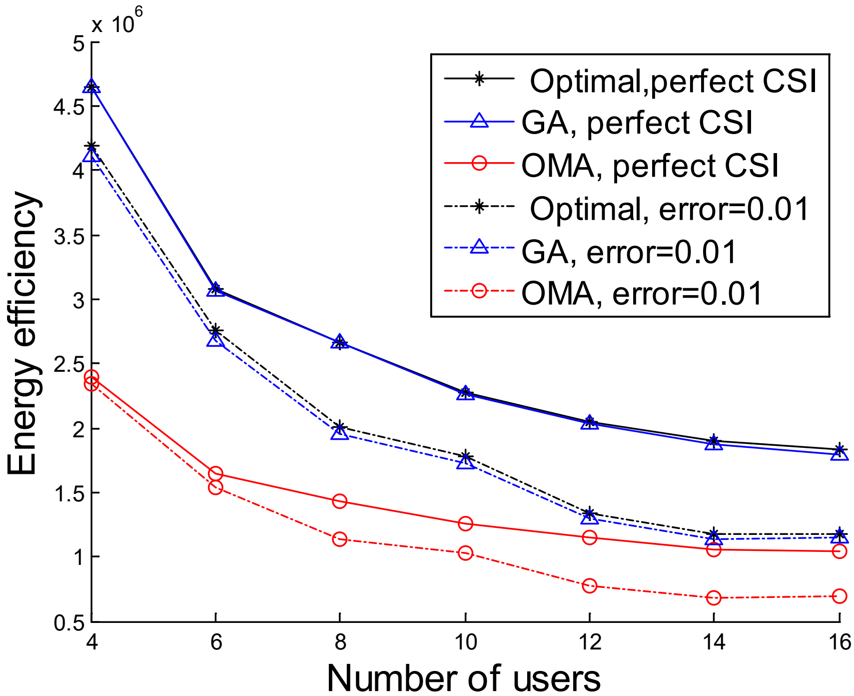

Figure 10. The impact of channel estimation error on the mmWave-NOMA system EE and mmWave-OMA system.

7. Conclusions

In this paper, we present a mixed-integer genetic algorithm (GA) to solve the EE optimization problem of a DL mmWave NOMA system with clustering subject to the various users' required SINRs. Then, we show that power allocation could not play an effective role in maximizing the proposed system's EE. The best system performance, in terms of energy efficiency, occurs when the allocating power satisfies the exact user-required data rate. Thus, the mixed-integer GA optimization problem is converted to an integer GA optimization problem to solve the best clustering that achieves the system's maximum EE. We determined the suitable minimum population size related to different numbers of system users: The population size increases dramatically during heavy traffic. In addition, the convergence of GA to reach the optimal result requires more repetitions (generations), and therefore the long execution time of GA at heavy traffic makes it more useful to prepare training data for deep learning algorithms where every cell is light, instead of real-time systems or dense cells at heavy traffic, because of its long execution time. Our results also show the outperformance of combining mmWave with NOMA as compared to the conventional orthogonal multiple access (OMA), where the proposed approach could improve the EE by more than 75%. The effect of the estimation error of CSI on the system performance was evaluated, where the results show that EE is degraded in the imperfect CSI case but the GA is still capable of determining almost the optimal solution under the same circumstances. The results reveal the ability of GAs to determine almost the optimal solution for different scenarios of user requirements. Since this study was limited to a single-cell model, implementing GA in more complex systems such as multiple cells and a higher number of cluster members will be investigated in future studies.

Author Contributions: Conceptualization, R.A., E.H. and K.D.; methodology, R.A. and E.H.; software, R.A.; validation, E.H. and K.D.; formal analysis, R.A., E.H. and K.D.; investigation, R.A., E.H. and K.D.; resources, R.A., E.H. and K.D.; data curation, R.A., E.H. and K.D.; writing—original draft preparation, R.A., E.H. and K.D.; writing—review and editing, E.H. and K.D.; visualization, R.A.; supervision, E.H. and K.D.; project administration, E.H. and K.D.; funding acquisition, E.H. and K.D. All authors have read and agreed to the published version of the manuscript.

Funding: This research was supported by the Ministry of Higher Education under the Fundamental Research Grant Scheme (FRGS/1/2020/TK0/UM/02/30).

Data Availability Statement: Not applicable.

Conflicts of Interest: The authors declare no conflict of interest.

References

1. Huang, T.; Yang, W.; Wu, J.; Ma, J.; Zhang, X.; Zhang, D. A Survey on Green 6G Network: Architecture and Technologies. *IEEE Access* **2019**, *7*, 175758–175768. [CrossRef]
2. Liu, X.; Ding, H.; Hu, S. Uplink Resource Allocation for NOMA-based Hybrid Spectrum Access in 6G-enabled Cognitive Internet of Things. *IEEE Internet Things J.* **2020**, *8*, 15049–15058. [CrossRef]
3. Zhu, L.; Xiao, Z.; Xia, X.; Wu, D.O. Millimeter-Wave Communications with Non-Orthogonal Multiple Access for B5G/6G. *IEEE Access* **2019**, *7*, 116123–116132. [CrossRef]
4. Wan, D.; Wen, M.; Ji, F.; Yu, H.; Chen, F. Non-Orthogonal Multiple Access for Cooperative Communications: Challenges, Opportunities, and Trends. *IEEE Wirel. Commun.* **2018**, *25*, 109–117. [CrossRef]
5. Ghosh, J.; Sharma, V.; Haci, H.; Singh, S.; Ra, I.H. Performance Investigation of NOMA versus OMA Techniques for mmWave Massive MIMO Communications. *IEEE Access* **2021**, *9*, 125300–125308. [CrossRef]
6. Chopra, R.; Murthy, C.R.; Suraweera, H.A.; Larsson, E.G. Analysis of Nonorthogonal Training in Massive MIMO under Channel Aging with SIC Receivers. *IEEE Signal Process. Lett.* **2019**, *26*, 282–286. [CrossRef]
7. Verma, S.; Kaur, S.; Khan, M.A.; Sehdev, P.S. Towards Green Communication in 6G-enabled Massive Internet of Things. *IEEE Internet Things J.* **2020**, *8*, 5408–5415. [CrossRef]
8. Mukherjee, A.; Goswami, P.; Khan, M.A.; Manman, L.; Yang, L.; Pillai, P. Energy Efficient Resource Allocation Strategy in Massive IoT for Industrial 6G Applications. *IEEE Internet Things J.* **2020**, *8*, 5194–5201. [CrossRef]
9. Viswanathan, H.; Mogensen, P.E. Communications in the 6G Era. *IEEE Access* **2020**, *8*, 57063–57074. [CrossRef]
10. Liu, P.; Li, Y.; Cheng, W.; Zhang, W.; Gao, X. Energy-Efficient Power Allocation for Millimeter Wave Beamspace MIMO-NOMA Systems. *IEEE Access* **2019**, *7*, 114582–114592. [CrossRef]
11. Gkonis, P.K.; Trakadas, P.T.; Sarakis, L.E. Non-Orthogonal Multiple Access in Multiuser MIMO Configurations via Code Reuse and Principal Component Analysis. *Electronics* **2020**, *9*, 1330. [CrossRef]
12. Chen, L.; Hu, B.; Xu, G.; Chen, S. Energy-Efficient Power Allocation and Splitting for mmWave Beamspace MIMO-NOMA With SWIPT. *IEEE Sens. J.* **2021**, *21*, 16381–16394. [CrossRef]
13. Zhai, D.; Zhang, R.; Cai, L.; Li, B.; Jiang, Y. Energy-Efficient User Scheduling and Power Allocation for NOMA-Based Wireless Networks with Massive IoT Devices. *IEEE Internet Things J.* **2018**, *5*, 1857–1868. [CrossRef]
14. Ahn, S.; Kim, J.; Park, S.Y.; Cho, S. Explaining Deep Learning-Based Traffic Classification Using a Genetic Algorithm. *IEEE Access* **2021**, *9*, 4738–4751. [CrossRef]
15. Liu, Y.; Wang, X.; Mei, J.; Boudreau, G.; Abou-Zeid, H.; Sediq, A.B. Situation-Aware Resource Allocation for Multi-Dimensional Intelligent Multiple Access: A Proactive Deep Learning Framework. *IEEE J. Sel. Areas Commun.* **2021**, *39*, 116–130. [CrossRef]
16. Zhang, H.; Fang, F.; Cheng, J.; Long, K.; Wang, W.; Leung, V.C.M. Energy-Efficient Resource Allocation in NOMA Heterogeneous Networks. *IEEE Wirel. Commun.* **2018**, *25*, 48–53. [CrossRef]
17. Wang, J.; Xu, H.; Fan, L.; Zhu, B.; Zhou, A. Energy-Efficient Joint Power and Bandwidth Allocation for NOMA Systems. *IEEE Commun. Lett.* **2018**, *22*, 780–783. [CrossRef]
18. Liu, G.; Wang, R.; Zhang, H.; Kang, W.; Tsiftsis, T.A.; Leung, V.C.M. Super-Modular Game-Based User Scheduling and Power Allocation for Energy-Efficient NOMA Network. *IEEE Trans. Wirel. Commun.* **2018**, *17*, 3877–3888. [CrossRef]
19. Zamani, M.R.; Eslami, M.; Khorramizadeh, M.; Ding, Z. Energy-Efficient Power Allocation for NOMA With Imperfect CSI. *IEEE Trans. Veh. Technol.* **2019**, *68*, 1009–1013. [CrossRef]
20. Song, X.; Dong, L.; Wang, J.; Qin, L.; Han, X. Energy Efficient Power Allocation for Downlink NOMA Heterogeneous Networks with Imperfect CSI. *IEEE Access* **2019**, *7*, 39329–39340. [CrossRef]
21. Fang, F.; Zhang, H.; Cheng, J.; Roy, S.; Leung, V.C.M. Joint User Scheduling and Power Allocation Optimization for Energy-Efficient NOMA Systems with Imperfect CSI. *IEEE J. Sel. Areas Commun.* **2017**, *35*, 2874–2885. [CrossRef]
22. Ding, Z.; Lei, X.; Karagiannidis, G.K.; Schober, R.; Yuan, J.; Bhargava, V.K. A Survey on Non-Orthogonal Multiple Access for 5G Networks: Research Challenges and Future Trends. *IEEE J. Sel. Areas Commun.* **2017**, *35*, 2181–2195. [CrossRef]
23. Ma, J.; Liang, C.; Xu, C.; Ping, L. On Orthogonal and Superimposed Pilot Schemes in Massive MIMO NOMA Systems. *IEEE J. Sel. Areas Commun.* **2017**, *35*, 2696–2707. [CrossRef]
24. Wei, Z.; Ng, D.W.K.; Yuan, J. Power-Efficient Resource Allocation for MC-NOMA with Statistical Channel State Information. In Proceedings of the 2016 IEEE Global Communications Conference (GLOBECOM), Washington, DC, USA, 4–8 December 2016; pp. 1–7.
25. Hou, T.; Liu, Y.; Sun, X.; Song, Z.; Chen, Y.; Hou, J. Massive NOMA Enhanced IoT Networks with Partial CSI. In Proceedings of the ICC 2020—2020 IEEE International Conference on Communications (ICC), Dublin, Ireland, 7–11 June 2020; pp. 1–6.

26. Xu, Y.; Cai, D.; Ding, Z.; Shen, C.; Zhu, G. Average Power Minimization for Downlink NOMA Transmission with Partial HARQ. In Proceedings of the 2018 IEEE Globecom Workshops (GC Wkshps), Abu Dhabi, United Arab Emirates, 9–13 December 2018; pp. 1–5.
27. Xu, P.; Yuan, Y.; Ding, Z.; Dai, X.; Schober, R. On the Outage Performance of Non-Orthogonal Multiple Access with 1-bit Feedback. *IEEE Trans. Wirel. Commun.* **2016**, *15*, 6716–6730. [CrossRef]
28. Spantideas, S.T.; Giannopoulos, A.E.; Kapsalis, N.C.; Kalafatelis, A.; Capsalis, C.N.; Trakadas, P. Joint energy-efficient and throughput-sufficient transmissions in 5G cells with deep Q-learning. In Proceedings of the 2021 IEEE International Mediterranean Conference on Communications and Networking (MeditCom), Athens, Greece, 7–10 September 2021; pp. 265–270.
29. Ding, Q.; Zhu, R.; Liu, H.; Ma, M.J.E. An overview of machine learning-based energy-efficient routing algorithms in wireless sensor networks. *Electronics* **2021**, *10*, 1539. [CrossRef]
30. Liu, R.; Lee, M.; Yu, G.; Li, G.Y. User Association for Millimeter-Wave Networks: A Machine Learning Approach. *IEEE Trans. Commun.* **2020**, *68*, 4162–4174. [CrossRef]
31. Zhang, H.; Zhang, H.; Long, K.; Karagiannidis, G.K. Deep Learning Based Radio Resource Management in NOMA Networks: User Association, Subchannel and Power Allocation. *IEEE Trans. Netw. Sci. Eng.* **2020**, *7*, 2406–2415. [CrossRef]
32. Pan, Y.; Yang, Y.; Li, W. A Deep Learning Trained by Genetic Algorithm to Improve the Efficiency of Path Planning for Data Collection with Multi-UAV. *IEEE Access* **2021**, *9*, 7994–8005. [CrossRef]
33. Celik, A.; Tsai, M.; Radaydeh, R.M.; Al-Qahtani, F.S.; Alouini, M. Distributed Cluster Formation and Power-Bandwidth Allocation for Imperfect NOMA in DL-HetNets. *IEEE Trans. Commun.* **2019**, *67*, 1677–1692. [CrossRef]
34. Wang, K.; Cui, J.; Ding, Z.; Fan, P. Stackelberg Game for User Clustering and Power Allocation in Millimeter Wave-NOMA Systems. *IEEE Trans. Wirel. Commun.* **2019**, *18*, 2842–2857. [CrossRef]
35. Li, L.; Ota, K.; Dong, M.; Verikoukis, C. Enabling 60 GHz Seamless Coverage for Mobile Devices: A Motion Learning Approach. In Proceedings of the 2018 IEEE Global Communications Conference (GLOBECOM), Abu Dhabi, United Arab Emirates, 9–13 December 2018; pp. 1–6.
36. Xie, S. Power allocation scheme for downlink and uplink NOMA networks. *IET Commun.* **2019**, *13*, 2336–2343. [CrossRef]
37. Ali, M.S.; Tabassum, H.; Hossain, E. Dynamic User Clustering and Power Allocation for Uplink and Downlink Non-Orthogonal Multiple Access (NOMA) Systems. *IEEE Access* **2016**, *4*, 6325–6343. [CrossRef]
38. Ali, M.S.; Hossain, E.; Al-Dweik, A.; Kim, D.I. Downlink Power Allocation for CoMP-NOMA in Multi-Cell Networks. *IEEE Trans. Commun.* **2018**, *66*, 3982–3998. [CrossRef]
39. Liu, Y.; Fang, X.; Xiao, M.; Mumtaz, S. Decentralized Beam Pair Selection in Multi-Beam Millimeter-Wave Networks. *IEEE Trans. Commun.* **2018**, *66*, 2722–2737. [CrossRef]
40. Zhou, T.; Zhao, J.; Qin, D.; Li, X.; Li, C.; Yang, L. Green Base Station Assignment for NOMA-Enabled HCNs. *IEEE Access* **2019**, *7*, 53018–53031. [CrossRef]
41. Vaezi, M.; Schober, R.; Ding, Z.; Poor, H.V. Non-Orthogonal Multiple Access: Common Myths and Critical Questions. *IEEE Wirel. Commun.* **2019**, *26*, 174–180. [CrossRef]
42. Zhao, J.; Yue, X.; Kang, S.; Tang, W. Joint Effects of Imperfect CSI and SIC on NOMA Based Satellite-Terrestrial Systems. *IEEE Access* **2021**, *9*, 12545–12554. [CrossRef]
43. Wei, H.; Li, S.; Quan, H.; Liu, D.; Rao, S.; Li, C.; Hu, J. Unified Multi-Objective Genetic Algorithm for Energy Efficient Job Shop Scheduling. *IEEE Access* **2021**, *9*, 54542–54557. [CrossRef]
44. Sai, Z.; Lu, C.; Jiang, S.; Shan, L.; James, C.; Xiong, N.N. Energy Management Optimization of Open-Pit Mine Solar Photothermal-Photoelectric Membrane Distillation Using a Support Vector Machine and a Non-Dominated Genetic Algorithm. *IEEE Access* **2020**, *8*, 155766–155782. [CrossRef]
45. Sun, X.; Yang, W.; Cai, Y. Secure Communication in NOMA-Assisted Millimeter-Wave SWIPT UAV Networks. *IEEE Internet Things J.* **2020**, *7*, 1884–1897. [CrossRef]
46. Mircea, E.; Chen-Ching, L.; Abdel-Aty, E. Genetic Algorithms. In *Advanced Solutions in Power Systems: HVDC, FACTS, and Artificial Intelligence*; IEEE: Piscataway, NJ, USA, 2016; pp. 845–902.
47. Deb, K. An efficient constraint handling method for genetic algorithms. *Comput. Methods Appl. Mech. Eng.* **2000**, *186*, 311–338. [CrossRef]
48. Deep, K.; Singh, K.P.; Kansal, M.L.; Mohan, C. A real coded genetic algorithm for solving integer and mixed integer optimization problems. *Appl. Math. Comput.* **2009**, *212*, 505–518. [CrossRef]